Available online at www.sciencedirect.com
ScienceDirect
Materials Science and Engineering C 27 (2007) 394–401
MATERIALS SCIENCE & ENGINEERING C
www.elsevier.com/locate/msec

Preparation of Zn-doped β-tricalcium phosphate (β-$Ca_3(PO_4)_2$) bioceramics

A. Cuneyt Tas [a,*], Sarit B. Bhaduri [b], Sahil Jalota [b]

[a] Department of Materials Science and Engineering, Mersin University, Mersin 33342, Turkey
[b] School of Materials Science and Engineering, Clemson University, Clemson 29634, USA

Available online 7 August 2006

Abstract

Pure β-tricalcium phosphate (β-TCP) and Zn-doped (600, 2900, 4100, 7000, 9300 and 10,100 ppm) β-TCP samples were prepared by using a wet chemical/coprecipitation synthesis technique, followed by calcination at 1000 °C in air. Precursor powders of the coprecipitation process were Ca-deficient nanoapatites (i.e., Ca/P molar ratio varying from 1.49 to 1.51) with needlelike but agglomerated particles of 30 nm thickness. In vitro culture tests performed by mouse osteoblast-like cells showed that the samples doped with 2900 to 4100 ppm Zn showed the highest cell viability (via Live/Dead counts), and with a further increase in the Zn-content towards 1 wt.% the number of dead cells in the well plates started to increase. Alkaline phosphatase (ALP) activity peaked for the β-TCP sample doped with 4100 pm Zn. The sample surface roughness, measured by non-contact profilometry, was also found to have an effect on the Live/Dead cell counts, and the highest cell viability encountered in this study corresponded to the surface with the least roughness.

Keywords: Bioceramic; Zinc; Tricalcium phosphate

1. Introduction

The mineralized portion of human bones and teeth essentially consists of nanosize and imperfect crystals of Ca-deficient, carbonated and alkali- and alkaline earth-doped biological apatites [1]. Bone apatites do not contain the β-tricalcium phosphate (β-TCP: β-$Ca_3(PO_4)_2$) phase. However, Mg-doped whitlockite, which can form in aqueous environments and structurally related to β-TCP, was found in human dental calculus [2] and in carious lesions [3,4]. Human bone depositing cells, namely the osteoblasts, are not programmed to synthesize the β-TCP phase in their physiological habitat, pH and temperature. β-TCP is a calcium phosphate ceramic of high solubility in comparison to Ca-hydroxyapatite (HA; $Ca_{10}(PO_4)_6(OH)_2$). The solubility activity product (K_{sp}) of β-TCP is 2.51×10^{-30} [5,6], whereas that of HA is 2.34×10^{-59} [7]. Owing to its significant solubility and ability of taking part in bone remodeling/turnover processes, β-TCP has become a bone substitute bioceramic in successful clinical use [8–10]. Wiltfang et al. [11] reported the in vivo resorbability (more than 95%) of β-TCP bioceramics in a minipig-tibia model observed over a period of 86 weeks.

The human nutritional need for zinc is small, but its role in growth and well-being is enormous, starting even before birth [12]. The entire body of a normal human weighing 70 kg may contain 1.4 to 2.3 g of zinc, and the recommended daily allowance of zinc is between 8 and 15 mg. Meats, seafood (especially oysters) and liver are the richest sources of zinc in food; brewer's yeast, milk, egg yolks, popcorn, beans, cocoa, and wheat germ also supply some zinc [13]. Zinc is found in body in small amounts in almost all tissues, however, the bones, teeth, and the pancreas contain slightly higher amounts than others. Human blood plasma contains approximately 1.5×10^{-2} mM of zinc [14]. Zinc is an essential trace element in a variety of cellular processes including DNA synthesis, behavioral responses, reproduction and virility, bone formation, bone growth and wound healing [15]. Zinc plays an important role in gene expression and in the regulation of cellular growth and differentiation [16], since it participates as a co-factor of more than 200 enzymes implied in the metabolism of nucleic acids, carbohydrates and proteins. Approximately 85% of the body store of zinc is found in skeletal muscles (55%) and bones (30%) [17]. The necessity of this trace element for bone growth was demonstrated by the observation that normal bone growth was retarded in animals that are zinc-deficient [18], and the addition of zinc to these deficient diets resulted in a stimulation of both bone growth and mineralization [19]. Zinc is the only

* Corresponding author. Fax: +90 324 361 0032.
E-mail address: actas@mersin.edu.tr (A. Cuneyt Tas).

0928-4931/$ - see front matter © 2006 Elsevier B.V. All rights reserved.
doi:10.1016/j.msec.2006.05.051

metal to be incorporated in all six enzyme classes of metalloenzymes, with the examples of oxidoreductase, transferase, hydrolase, lyase, isomerase, and ligase activity [20]. Important bone enzymes, including alkaline phosphatase (ALP) and carbonic anhydrase are zinc metalloenzymes, and tartrate-resistant acid phosphatase (TRAP) is strongly inhibited by zinc [21,22]. In brief, zinc deficiency has been associated with skeletal growth retardation, reduced ALP activity [18], reduced premenopausal bone mass [23] and postmenopausal osteoporosis [24]. Clinical trials have also shown that zinc supplementation inhibits postmenopausal bone loss [25]. Zinc has been implicated in bone formation, mineralization [26], and the stimulation of ALP activity in calvarial organ cultures [18,27], osteoblast-like cell cultures [28–30], as well as the stimulation of the bone DNA synthesis via the activation of bone DNA polymerase [31]. Zinc deficiency, on the other hand, were recently shown to cause about 300% increase in programmed cell death (or apoptosis) in mice in a variety of kinds of cells [32], and insufficient zinc initiated apoptosis in hepatocytes, glioma, kidney, monocytes, fibroblasts, and testicular cells.

To the best of our knowledge, a thorough investigation on the synthesis of Zn-doped HA and/or TCP bioceramics has a rather short history. Fuierer et al. [33] and Bigi et al. [34] performed the pioneering studies in this field, which reported the inhibiting effect of zinc on HA crystal growth in aqueous systems. A later report by Bigi et al. [35] attempted to synthesize Zn-doped β-TCP bioceramics at Zn dopant levels from 2.5 to 20 mol%, with increments of 2.5 mol% over this range. Bigi et al. [35] first prepared single-phase β-TCP ceramics by calcining a stoichiometric powder mixture of $CaHPO_4{\cdot}2H_2O$ and $CaCO_3$ at 1000 °C for 15 h. To produce the Zn-doped β-TCP bioceramics, Bigi et al. [35] mixed the phase-pure β-TCP powders with those of α-$Zn_3(PO_4)_2$ and calcined the resultant mixtures at 1000 °C for 15 h. Bigi et al. [35] concluded that the small Zn ion (0.074 nm) readily replaced the larger Ca ion (0.099 nm) in the β-TCP structure (rhombohedral, space group R*3c*), causing a steady and monotonic decrease in the *a*-axis of the unit cell from 10.44 to 10.325 Å, while causing a slight decrease in the *c*-axis length from 37.41 to 37.25 Å, with isomorphic Zn substitution from 2.5 to 20 mol% over the Ca-sites. LeGeros [36,37] has been the first to report the formation of TCP phase (together with needlelike apatite crystals) in aqueous solutions containing zinc. The last 5 years have seen a number of publications [38–51] coming from the laboratory of Dr. Atsuo Ito, all concerning with the synthesis and/or in vitro–in vivo testing of Zn-containing calcium phosphate ceramics. In some studies of the Ito group, the ZnTCP samples (to be later blended with HA powders) were prepared by the $Ca(OH)_2$–H_3PO_4 neutralization route with the addition of zinc nitrate into those solutions to obtain 10 to 30 mol% Zn doping [39], while in some studies by Layrolle et al. [52] a sol–gel route, which used $Ca(OEt)_2$ (obtained from the reaction of Ca metal shots and ethyl alcohol), H_3PO_4 and Zn-acetate, was employed to synthesize the samples. The Ito group synthesized numerous calcium phosphate samples by doping Zn starting from 600 ppm level up to 10–20 mol% [48]. However, most of the studies of this group were focused more on the in vivo and in vitro testing of ZnTCP–HA biphasic samples. Therefore, the reports originating from the Ito group which focused only on the testing of Zn-doped β-TCP (i.e., without any HA) [41,45,50,51] are in direct relevance with the present study. However, in these studies the following points can be underlined: (i) their powder samples were produced by using the $Ca(OH)_2$–H_3PO_4–Zn-nitrate synthesis route [41,45,50,51], (ii) when the authors were adding 12 mol% Zn, their samples were reported to contain the phase of $CaZn_2(PO_4)_2$ [51], (iii) the authors first synthesized 10 mol% ZnTCP powders and then mixed those in a mortar with pure β-TCP powders to obtain 0.28%, 2.56%, 5.0%, 7.47%, and 10.5% Zn-containing ZnTCP samples after calcination at 1000 °C [45], (iv) when the authors were preparing the so-called 12 wt.% Zn-containing ZnTCP samples, they reported to have the secondary phases of $Ca_{2.7}Zn_{0.3}(PO_4)_2$ and $CaZn_2(PO_4)_2$ [41,50], (v) the authors never cited the important work of Bigi et al. [35] and compared their findings with those reported before, (vi) the authors did not study the low end of the Zn-doping range. The goals of the present study can be briefly stated as follows; (i) to develop an aqueous coprecipitation process (incorporating a calcination step; at 1000 °C) for synthesizing Zn-β-TCP samples with Zn levels ranging from 600 ppm to about 1.0 wt.% to eliminate the need for physical mixing of more than one powders to produce Zn-doped calcium phosphate bioceramics, (ii) to characterize the samples by using XRD, FTIR, TGA, ICP-AES, density and surface profilometry measurements, (iii) to test the cytotoxicity and ALP (alkaline phosphatase) activity of the Zn-β-TCP samples (600, 2900, 4100, 7000, 9300 and 10,100 ppm Zn) by using rat osteoblast-like cells.

2. Experimental procedure

2.1. Sample preparation

$Ca(NO_3)_2{\cdot}4H_2O$ (>99.5%, Fisher), $NH_4H_2PO_4$ (>99.5%) and $Zn(NO_3)_2{\cdot}6H_2O$ (>99.9%) were the starting chemicals used in powder synthesis. α-$Zn_3(PO_4)_2$ powder (TZP; 99.995%, #13013) was provided by Alfa-Aesar Inc. Briefly, $NH_4H_2PO_4$ was dissolved in deionized water in a glass beaker, and in a separate beaker $Ca(NO_3)_2{\cdot}4H_2O$ and $Zn(NO_3)_2{\cdot}6H_2O$ were dissolved in proper amounts. Ca-Zn-nitrate mixed solution was then added at once into the phosphate solution, the slight turbidity instantly observed was eliminated by adding few drops of concentrated HNO_3 (69 vol.%, Fisher) which also brought the solution pH down to 3±0.1 from around 4, and therefore, a clear solution was obtained. This solution was stirred (200 rpm) at 37 °C for 2 h to ensure a homogeneous mixture, followed by rapidly adding about 50 ml of a concentrated NH_4OH (29% NH_3, Merck) solution to obtain precipitation and a stable pH value of around 9.2±0.2 again at 37 °C. The opaque solution was stirred for 1 h. Formed precipitates were filtered (paper No. 42) via a Buechner funnel, washed with 4 l of water, and then dried at 90 °C for 12 h in air in glass dishes. Dried powders, which were free of hard agglomerates, were only lightly ground in an agate mortar by a pestle. Precursor powders were

uniaxially pressed (3580 kg/cm^2) into 1.5-mm-thick, 1.27-cm-diameter pellets in steel molds and then calcined in air at 1000 °C for 6 h in clean Al_2O_3 boats or crucibles (heating/cooling rate: 3 °C/min). TZP powders were also pressed into pellets and later calcined in the way as described above. The details of powder syntheses were given in Table 1, in which the samples of interest were named according to their experimentally-determined (by ICP-AES) ppm Zn values after calcination.

2.2. Characterization

Chemical analyses of powder (both precursor and calcined) samples were performed by ICP-AES (Model 61E, Thermo Electron, Madison, WI). During the ICP-AES analyses, 50 mg portions of powder samples were dissolved in 5 ml of concentrated HNO_3 solution. Surface roughness of the calcined Zn-β-TCP pellets were measured, prior to cell culture tests, by a non-contacting surface profilometer (NT-2000, Wyko, Tucson, AZ) at the magnification of 25× and over a 164×215 μm field of view. In profilometry, R_t was the maximum height minus the minimum height in the field of view, whereas R_z was the average of 5 highest peaks minus the average of 5 lowest valleys. Bulk densities of the calcined pellets (repeated 5×) were measured by using a pycnometer (AccuPyc 1330, Micromeritics, Norcross, GA) with He gas.

For the phase analyses of powder samples an X-ray diffractometer (XRD; XDS 2000, Scintag Corp., Sunnyvale, CA) was used (Cu K_α radiation at 40 kV and 30 mA, with a step size of 0.03° and preset time of 1 s at each step). Samples were also analyzed by FTIR (Nicolet 550, Thermo-Nicolet, Woburn, MA). Scanning electron microscopy (FE-SEM; S-4700, Hitachi, Tokyo) was used in the secondary electron mode with an acceleration voltage of 5 kV to image the samples.

2.3. In vitro cell culture tests

Statistical sample size (i.e., n) was 16 in the entirety of the cell culture tests. 7F2 rat osteoblast-like cells (CRL-12557, American Type Culture Collection, Rockville, MD) were grown on 75 cm^2 culture flasks at 37 °C and 50% CO_2 in α-MEM with 2 mM 1-glutamine and 1 mM sodium pyruvate without ribonucleosides and deoxyribonucleosides, augmented by 10% FBS. The culture medium was changed every other day until the cells reached a confluence of 90–95%, as determined visually with an inverted microscope. The cells then were passaged using trypsin (2.5 g/l)/EDTA (25 mM) solution (Sigma-Aldrich Corp., St. Louis, MO, USA). The obtained cells were then seeded at a concentration of 3500 cells/well on 0.14 cm^3 samples for various assays. Cell viability and alkaline phosphatase activity measurements were performed after 72 h. The cell viability assessment was performed using Live/Dead® Viability/Cytotoxicity Kit (L-3224, Molecular Probes, Eugene, OR). A working solution is prepared by mixing 5 μl aliquot of Component A (4 mM calcein AM solution in DMSO) to 10 ml of 4 mM EthD-1 solution (20 μl of the Component B to 10 ml of DPBS). 100 μl of this working solution was added to the cell-containing samples along with 100 μl of cell-containing media. Samples were incubated at room temperature for 30–45 min. After the prescribed time period, the fluorescence values were recorded at 494/517 nm for live cells and 528/617 nm for dead cells by using a standard curve obtained by seeding different number of cells in different wells. The alkaline phosphatase (ALP) activity was determined using the ALP concentration and the cell extracted protein concentration. The ALP concentration was calculated using Enzymatic Assay of Phosphatase Alkaline Kit (EC 3.1.3.1, Sigma-Aldrich Corp., St. Louis, MO, USA). A working reagent was prepared by first mixing 2.7 ml of Reagent A (1.0 M Diethanolamine Buffer with 0.50 mM Magnesium Chloride) with 0.30 ml of Reagent B (150 mM *p*-Nitrophenyl Phosphate Solution (pNPP)) and then mixing the mixture with 0.10 ml of cell-containing media. 100 μl of this solution was added to each well and thoroughly mixed and incubated at 37 °C for 30 min. Following incubation, the absorbance was recorded at 405 nm with the spectrophotometer at room temperature. The standard curve was obtained by plotting the absorbance measured at 405 nm for certain concentration against the concentration in μg/ml. ALP concentration of each sample was then determined using this standard curve and is expressed as μg pNP/ml. The cell extracted protein concentration was determined in a two-step procedure, first the protein was extracted using M-PER™ Mammalian Protein Extraction reagent and then this extracted protein was measured using BCA™ Protein Assay Kit. The cell samples were lysed by adding 200 μl of M-PER™ Reagent to each well plate and then shaked for 5 min. Lysate was collected and transferred to microcentrifuge tubes, followed by centrifugation at 4000×g for 10 min to pellet the cell debris. The supernatant was transferred to clean tubes for analyzing the protein concentration. To

Table 1
Powder synthesis procedure

Sample[a] (ppm Zn)	$NH_4H_2PO_4$ [in 225 ml H_2O]	$Ca(NO_3)_2{\cdot}4H_2O+Zn(NO_3)_2{\cdot}6H_2O$ [in 600 ml H_2O]	ICP-AES results[b]			
			P (%)	Ca (%)	Zn (ppm)	Ca/P
Zn-600	22.4424 g	[69.0483 g+0.2763 g]	22.14	42.85	600	1.496
Zn-2900	22.4424 g	[68.9212 g+0.4362 g]	21.58	42.52	2900	1.513
Zn-4100	22.4424 g	[68.7205 g+0.6900 g]	18.94	36.46	4100	1.488
Zn-7000	22.4424 g	[68.3422 g+0.9651 g]	19.95	38.85	7000	1.505
Zn-9300	22.4424 g	[68.1447 g+1.3140 g]	18.78	36.25	9300	1.492
Zn-10,100	22.4424 g	[67.9471 g+1.6631 g]	20.16	38.92	10,100	1.493

[a] ppm Zn in β-TCP, measured by ICP-AES in powder samples calcined at 1000 °C for 6 h.
[b] ICP-AES analyses of powder samples calcined at 1000 °C for 6 h.

measure the protein amount, a working reagent (WR) was prepared by mixing 50 parts of BCA™ Reagent A with 1 part of BCA™ Reagent B (50:1, Reagent A/B). 200 µl of the above-mentioned WR was added to each well and thoroughly mixed. Following mixing, the well plate was covered and incubated at 37 °C for 30 min. The absorbance at 562 nm was measured with the spectrophotometer at room temperature. A standard curve was prepared by plotting the average blank-corrected 562 nm measurement for each BSA standard versus its concentration in µg/ml. Cell extracted protein concentration was then determined by using this standard curve and is expressed as µg/ml. The ALP activity was then calculated as follows; ALP activity = [(µg pNP)/139]/µg(cell extracted protein) = µmol pNPP/µg cell protein. Osteoblast attachment/proliferation on the pellets was studied using SEM. Cells were first fixed by using 3.5% glutaraldehyde, and then dehydrated through sequential washings in 50%, 70%, 95% ethanol solutions and 2 times in 100% ethanol. Samples were then critical point-dried, prior to sputter-coating with a thin layer of Pt.

3. Results and discussion

The pure and Zn-doped precursor powders of this study gave the same XRD pattern as shown in Fig. 1A, which belonged to that of Ca-deficient apatitic calcium phosphate (CDHA: $Ca_9(HPO_4)(PO_4)_5OH$). Yubao et al. [53] previously called this phase as apatite-TCP and gave a full account of its crystal structure. Rietveld refinement of the structure of CDHA was performed by Ivanova et al. [54] and Tas et al. [55]. Gibson et al. [56], on the other hand, studied the thermal transformation of CDHA into β-TCP. FTIR spectra of the precursor powders were given in Fig. 1B, while the ICP-measured Zn levels (in ppm) were indicated on the diagram. The vibrations indicated in Fig. 1B with arrows denoted the OH vibrations, whereas the rest indicated the characteristic PO_4^{3-} and CO_3^{2-} vibrations [56].

It should hereby be noted that there was a difference between the ppm Zn levels achieved in the powders before and after calcination (see Table 1). This was believed to be due to the difference(s) in surface adsorbed or in hydroxide-form Zn (i.e., in precursor powders) and the structure-assimilated Zn ions (i.e., after heating). Calcination, and therefore, the solid-state diffusion apparently had a certain effect on the stabilization of the final Zn content of the samples. According to the ICP-AES results of the precursors and the calcined samples, vaporization of Zn was not observed during calcination. TGA traces of the precursors (Fig. 1C) showed, from RT to around 500 °C, an initial weight loss between 4% and 9%, which corresponded to the loss of surface adsorbed water and probably some residual ammonium and nitrate ions [54]. The unique shoulder observed at around 720 °C in Fig. 1C represented the volatilization of

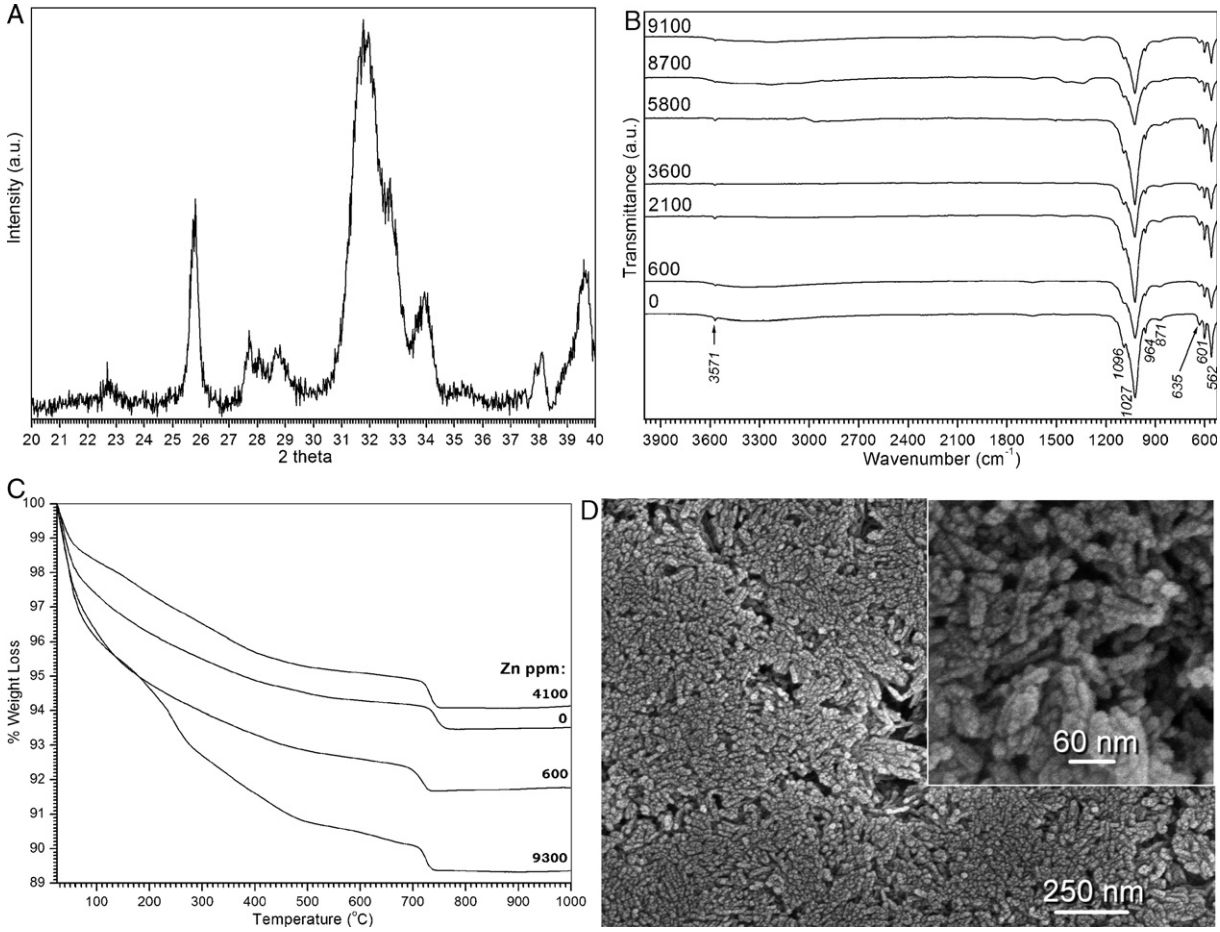

Fig. 1. (A) XRD spectra of the precursors. (B) FTIR spectra of the precursors. (C) TGA traces of select precursors. (D) SEM micrographs of precursors.

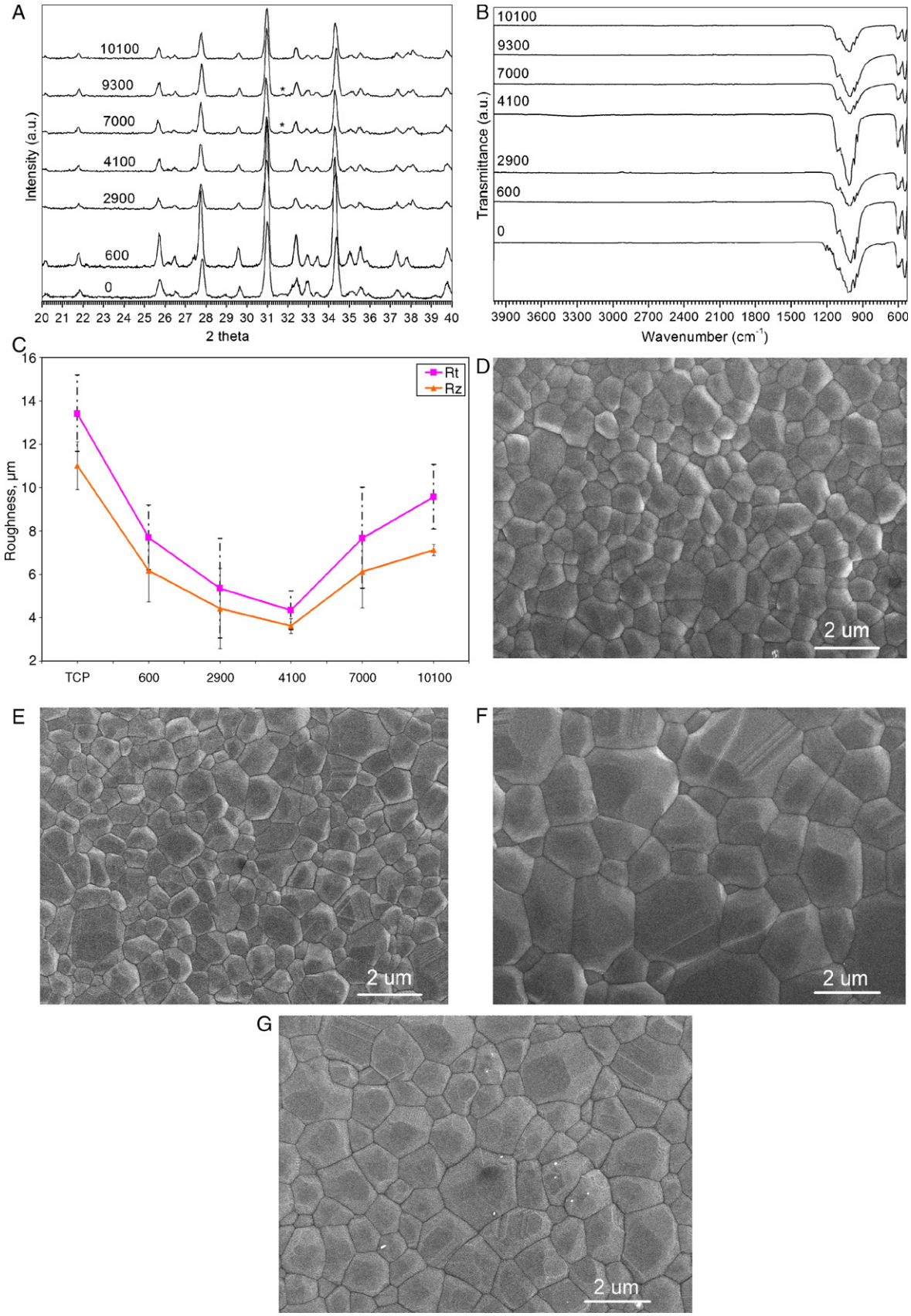

Fig. 2. (A) XRD spectra of calcined samples. (B) FTIR spectra of calcined samples. (C) Surface profilometry of calcined samples. (D) SEM micrograph of pure β-TCP pellet. (E) SEM micrograph of 2900 ppm Zn-βTCP. (F) SEM micrograph of 4100 ppm Zn-βTCP. (G) SEM micrograph of 10,100 ppm Zn-βTCP.

Table 2
Bulk densities of Zn-doped β-TCP pellets

Zn (ppm)	Density (g/cm^3)	Standard deviation
0	3.049	0.022
600	3.024	0.027
2900	3.028	0.016
4100	3.068	0.028
7000	2.997	0.013
9300	2.992	0.017
10,100	2.945	0.021

carbonate ions. Carbonated nature of these precursor powders were also detected by their FTIR spectra of Fig. 1B. It was difficult to find a direct correlation between the TGA weight loss behavior and the Zn-dopant level. The high-magnification SEM micrographs given in Fig. 1D were recorded directly on the surface of a green pellet prepared from 8700 ppm Zn-containing TCP precursors, and the same morphology was also observed on 600 ppm Zn-containing precursors (data not shown). Micrographs of Fig. 1D confirmed (as did Fig. 1A) the nanocrystalline nature of these precursors, and the powders consisted of acicular particles of about 100 nm long and 30 nm thick. TEM studies are underway. Apparently, uniaxial pressing of those powders into a pellet at 3580 kg/cm^2 forced them to pack closely.

Calcination of the pure and Zn-doped precursor powders at 1000 °C resulted in the complete transformation of CDHA into β-TCP and Zn-doped β-TCP. The Zn-content and Ca/P molar ratio of the calcined pellets were depicted in Table 1. The XRD (Fig. 2A, Zn-content in ppm values were indicated on the traces) and FTIR (Fig. 2B) spectra of the calcined samples confirmed the formation of β-TCP. The small extraneous peaks in Fig. 2A, labeled by asterisks in the traces of 7000 and 9300 ppm Zn-containing samples, corresponded to the very strong 211 reflection of the HA phase. In reproduction runs for the samples these peaks were not observed, but we decided to report here the original data. This probably showed an inherent limitation of our synthesis procedure in producing 100% pure β-TCP samples. Calcination of the precursors in an air atmosphere (at uncontrolled relative humidity levels from one experiment to the other) may also be influential on this point of HA formation. Surface profilometry data shown in Fig. 2C indicated an interesting decrease in surface roughness at around 2900 and 4100 ppm Zn-content, with increasing or decreasing Zn-dopant level surface roughness increased. The surface morphology of a pure β-TCP calcined pellet was given in Fig. 2D, grain sizes ranged from 350 nm to 2 μm. However, the grain size distribution in 2900 and 4100 ppm Zn-β-TCP samples were quite different from that of pure β-TCP, as shown in Fig. 2E and f, respectively. The significant increase in the average grain size of the 4100 ppm Zn-β-TCP sample should also explain for the dip in the surface profilometry results given in Fig. 2C. The slight decrease in the average grain size in the 10,100 ppm Zn-β-TCP sample (Fig. 2G) was interesting to note. These data showed that Zn was also an effective dopant in altering the grain boundary area in this new class of β-TCP samples. The progressive Zn doping caused a decrease in the bulk density of the pellets calcined at 1000 °C, as shown in Table 2. The density data of Table 2 represented densification in excess of 95% of the theoretical density of β-TCP. The 600 ppm Zn-β-TCP sample had the formula $Ca_{2.997}Zn_{0.003}(PO_4)_2$, whereas the formula for the 10,100 ppm sample was $Ca_{2.952}Zn_{0.048}(PO_4)_2$. The TZP pellet, which was used as a control in the cell culture tests, showed the polymorphic transformation from the α-(ICDD PDF 29-1390) to the β-form (ICDD PDF 30-1489) upon calcination at 1000 °C (XRD and FTIR data not shown). This polymorphic transformation in TZP was known to occur above 942 °C.

The results of culture tests with mouse osteoblast-like cells were summarized by the histograms given in Fig. 3A (Live/Dead cytotoxicity) and B (ALP activity). Taking into consideration the rather significant length of the error bar on the 2900 ppm Zn sample in Fig. 3A and the highest ALP activity observed for 4100 ppm Zn sample (Fig. 3B), it can be stated that the maximum proliferation of the osteoblast-like cells was recorded on the 4100 ppm Zn-β-TCP sample of this study. It will also be interesting to couple this finding with the fact that the minimum surface roughness (Fig. 2C) and the maximum bulk density (Table 2) values of this study were observed for the very same 4100 ppm Zn-β-TCP sample. β-TZP was found to be a perfectly cytotoxic material (Fig. 3A). It also became apparent that, in comparison to pure β-TCP, the presence of Zn especially at the dopant levels of 2900, 4100 and 7000 ppm significantly

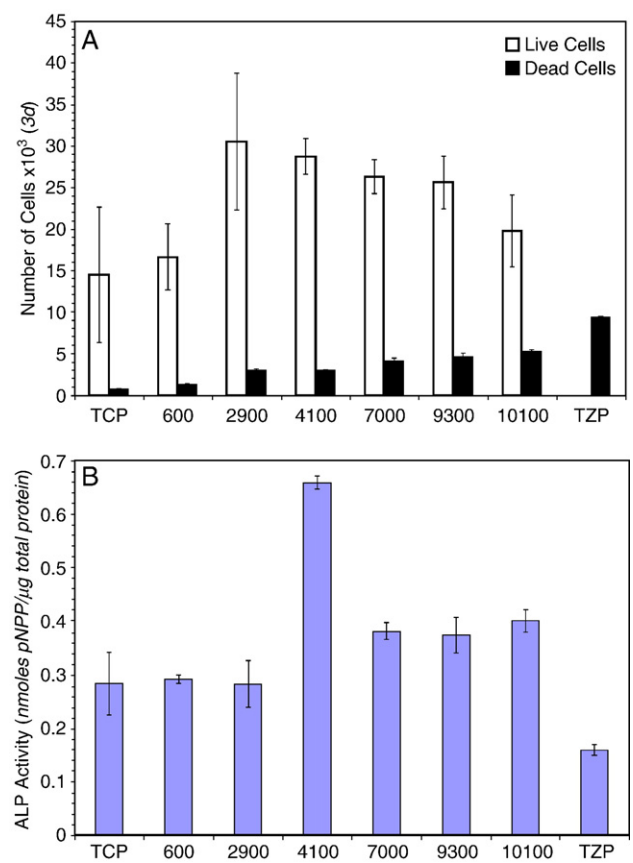

Fig. 3. (A) Live/Dead (cytotoxicity) data for Zn-β-TCP. (B) ALP activity data for Zn-β-TCP.

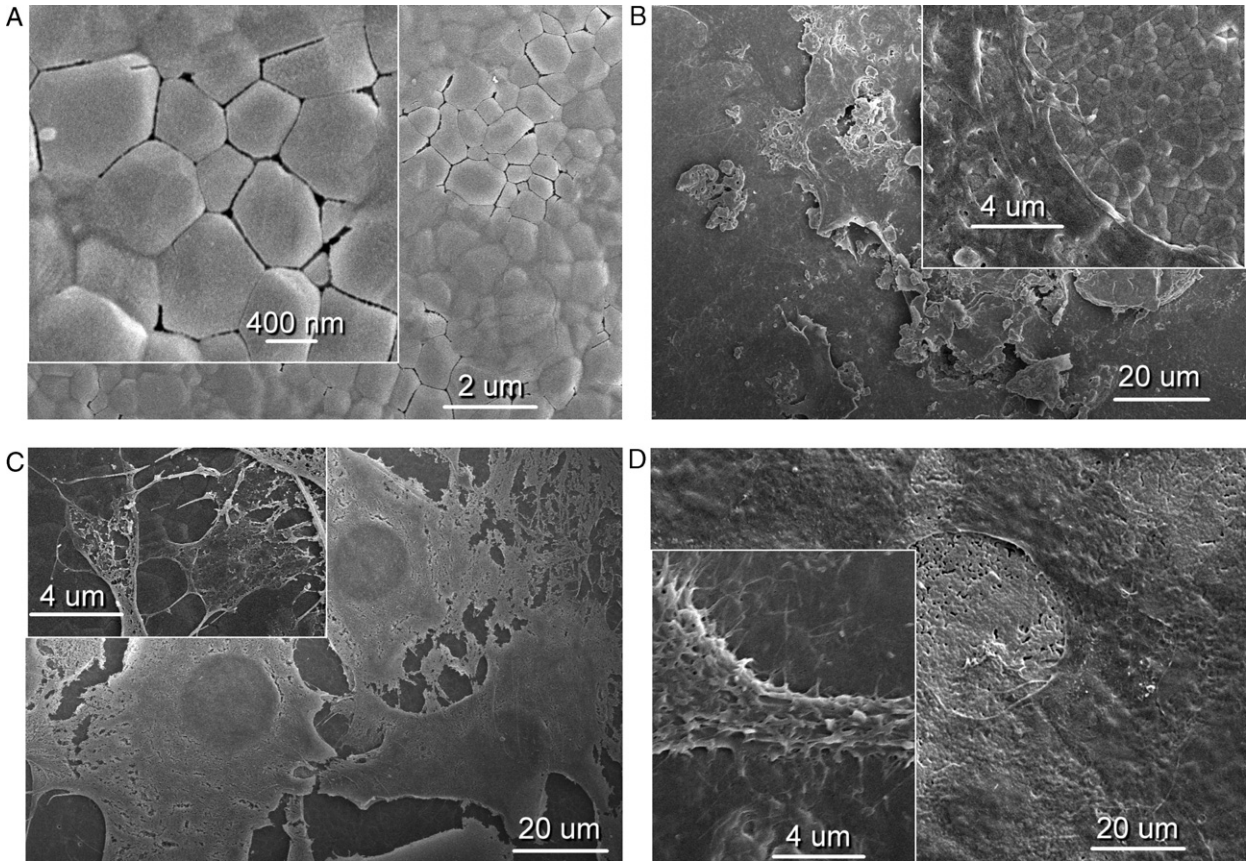

Fig. 4. (A) Osteoblasts on pure β-TCP pellet. (B) Osteoblasts on 2900 ppm Zn-β-TCP pellet. (C) Osteoblasts on 4100 ppm Zn-β-TCP pellet. (D) Osteoblasts on 7000 ppm Zn-β-TCP pellet.

increased the osteoblastic activity (Fig. 3A and B) [57]. This point is in very well agreement with the previous literature cited in Section 2. The attachment and spreading of osteoblasts on various Zn-β-TCP pellets were imaged by SEM and given in Fig. 4. On pure β-TCP pellets, osteoblasts spread like a thin, electron-translucent membrane so that the underlying grains were still visible (Fig. 4A). The erosion of the grain boundaries (Fig. 4A) during the cell culture tests may indicate that there might have been a highly soluble amorphous CaP grain boundary phase which dissolved under the alkaline phosphatase enzyme activity. The 2900 ppm Zn-containing sample surfaces (Fig. 4B) showed a high degree of osteoblast coverage, and the inset in Fig. 4B displayed quite a significant degree of cell spreading. The cell nuclei became visible even by the SEM images on 4100 ppm Zn-containing β-TCP samples (Fig. 4C). Typically, such imaging of cell nuclei could be achieved by using fluorescent microscopy together with special histological staining practices. In this case (i.e., 4100 ppm Zn), the cells were also proliferating into cytoskeletal stress fibers beyond extending their filopodia. When the Zn-content was increased to 7000 ppm (Fig. 4D), the cell attachment and spreading was still at quite high levels. On the surfaces of β-TZP samples, it was not possible to find even a single cell to image by the SEM, confirming the cytotoxicity results of Fig. 3A.

Although the sample preparation routes of the two studies differed from one another significantly, the findings of the present work enhanced those of Ito et al. [45], especially at the ppm level Zn-doping into β-TCP. In vivo resorbability of the samples of this study must be tested. The search for more reliable ways of Zn-doping in calcium phosphates (HA, TCP or biphasic HA–TCP) and the in vitro and in vivo characterization of the resultant samples seems to be an exciting field of biomaterials research [58–62].

4. Conclusions

(1) Aqueous coprecipitation was used for synthesizing ppm level Zn-doped β-TCP precursor nanopowders. This method was suitable to produce 600, 2900, 4100, 7000, 9300 and 10,100 ppm Zn-containing β-TCP samples after calcination at 1000 °C for 6 h in an air atmosphere.

(2) Zinc was found to influence the grain growth characteristics and densification of β-TCP samples. 4100 ppm Zn-doped β-TCP sample was observed to have the highest bulk density within the range of dopant levels studied in this work.

(3) In vitro cell culture tests performed with mouse osteoblast-like cells showed the significant effect of ppm level presence of Zn in β-TCP samples in enhancing the osteoblastic activity, in direct comparison to pure β-TCP and β-TZP. The Live/Dead cytotoxicity counts and

alkaline phosphatase activity data were collected for all the samples.

(4) Live/Dead counts were peaked for the 2900 ppm Zn-β-TCP samples, whereas the ALP activity was found to be the highest for the 4100 ppm Zn-containing β-TCP samples.

Acknowledgements

This work was partially supported by an NSF Grant No. 0522057.

References

[1] A.S. Posner, E.D. Eanes, R.A. Harper, I. Zipkin, Arch. Oral Biol. 8 (1963) 549.
[2] S.W. Leung, A.T. Jensen, Int. Dent. J. 8 (1958) 613.
[3] H. Llory, R.M. Frank, Actual. Odonto-Stomatol. 88 (1969) 507.
[4] R.Z. LeGeros, Calcium Phosphates in Oral Biology and Medicine, Karger, New York, 1991.
[5] R. Tang, W. Wu, M. Haas, G.H. Nancollas, Langmuir 17 (2001) 3480.
[6] W. Wu, R. Tang, M. Haas, G.H. Nancollas, J. Colloid Interface Sci. 244 (2001) 347.
[7] H. McDowell, W.E. Brown, J.R. Sutter, Inorg. Chem. 10 (1971) 1638.
[8] H. Yuan, J.D. DeBruijn, Y. Li, J. Feng, Z. Yang, K. deGroot, X. Zhang, J. Mater. Sci., Mater. Med. 12 (2001) 7.
[9] R.D.A. Gaasbeek, H.G. Toonen, R.J. van Heerwaarden, P. Buma, Biomaterials 26 (2005) 6713.
[10] R.Z. LeGeros, Clin. Orthop. Relat. Res. 395 (2002) 81.
[11] J. Wiltfang, H.A. Merten, K.A. Schlegel, S.S. Mosgau, F.R. Kloss, S. Rupprecht, P. Kessler, J. Biomed. Mater. Res. 63B (2002) 115.
[12] M. Merialdi, L.E. Caulfield, N. Zavaleta, A. Figuerota, K.A. Costigan, F. Dominici, J.A. Dipietro, Am. J. Clin. Nutr. 79 (2004) 826.
[13] E.W. Murphy, B.W. Willis, B.K. Watt, J. Am. Diet. Assoc. 66 (1975) 345.
[14] S. Cin, E. Unal, A. Pamir, B. Kologlu, A.O. Cavdar, J. Trace Elem. Exp. Med. 14 (2001) 31.
[15] D.G. Barceloux, J. Toxicol., Clin. Toxicol. 37 (1999) 279.
[16] M. Hambidge, J. Nutr. 130 (2000) 1344.
[17] D. Chen, L.C. Waite, W.M. Pierce, Biol. Trace Elem. Res. 61 (1998) 9.
[18] G. Oner, B. Bhaumick, R.M. Bala, Endocrinology 114 (1984) 1860.
[19] M. Yamaguchi, H. Oishi, Y. Suketa, Biochem. Pharmocol. 36 (1987) 4007.
[20] B.L. Vallee, K.H. Falchuk, Physiol. Rev. 73 (1993) 79.
[21] A. Togari, S. Arakawa, M. Arai, S. Matsumoto, Gen. Pharmacol. 24 (1993) 1133.
[22] W.R. Holloway, F.M. Collier, R.E. Herbst, J.M. Hodge, G.C. Nicholson, Bone 19 (1996) 137.
[23] R.M. Angus, P.N. Sambrook, N.A. Pocock, J.A. Eisman, Bone Miner. 4 (1988) 265.
[24] M. Hertzberg, J. Foldes, R. Steinberg, J. Menczel, J. Bone Miner. Res. 5 (1990) 251.
[25] P.D. Saltman, L.G. Strause, J. Am. Coll. Nutr. 12 (1993) 384.
[26] D.L. Bougle, J.P. Sabatier, G.G. Souquieres, F.G. Metz, D. Laroche, P. Jauzac, F. Bureau, J. Trace Elem. Med Biol. 18 (2004) 17.
[27] M. Yamaguchi, A. Igarashi, S. Uchiyama, J. Health Sci. 50 (2004) 75.
[28] M. Yamaguchi, H. Miwa, Pharmacology 42 (1991) 230.
[29] Z.J. Ma, M. Yamaguchi, J. Bone Miner. Metab. 18 (2000) 264.
[30] Z.J. Ma, M. Yamaguchi, J. Bone Miner. Metab. 19 (2001) 38.
[31] Z.J. Ma, M. Yamaguchi, Calcif. Tissue Int. 69 (2001) 158.
[32] P.J. Fraker, J. Nutr. 135 (2005) 359.
[33] T.A. Fuierer, M. LoRe, S.A. Puckett, G.H. Nancollas, Langmuir 10 (1994) 4721.
[34] A. Bigi, E. Foresti, M. Gandolfi, M. Gazzano, N. Roveri, J. Inorg. Biochem. 58 (1995) 49.
[35] A. Bigi, E. Foresti, M. Gandolfi, M. Gazzano, N. Roveri, J. Inorg. Biochem. 66 (1997) 259.
[36] R.Z. LeGeros, Caries Res. 31 (1997) 434.
[37] R.Z. LeGeros, C.B. Bleiwas, M. Retino, R. Rohanizadeh, J.P. LeGeros, Am. J. Dent. 12 (1999) 65.
[38] N. Kanzaki, K. Onuma, G. Treboux, S. Tsutsumi, A. Ito, J. Phys. Chem., B 104 (2000) 4189.
[39] A. Ito, K. Ojima, H. Naito, N. Ichinose, T. Tatseishi, J. Biomed. Mater. Res. 50 (2000) 178.
[40] H. Kawamura, A. Ito, S. Miyakawa, P. Layrolle, K. Ojima, N. Ichinose, T. Tateishi, J. Biomed. Mater. Res. 50 (2000) 184.
[41] M. Otsuka, S. Marunaka, Y. Matsuda, A. Ito, P. Layrolle, H. Naito, N. Ichinose, J. Biomed. Mater. Res. 52 (2000) 819.
[42] N. Kanzaki, K. Onuma, G. Treboux, S. Tsutsumi, A. Ito, J. Phys. Chem., B 105 (2001) 1991.
[43] A. Ito, H. Kawamura, M. Otsuka, M. Ikeuchi, H. Ohgushi, K. Ishikawa, K. Onuma, N. Kanzaki, Y. Sogo, N. Ichinose, Mater. Sci. Eng., C 22 (2002) 21.
[44] K. Ishikawa, Y. Miyamoto, T. Yuasa, A. Ito, M. Nagayama, K. Suzuki, Biomaterials 23 (2002) 423.
[45] A. Ito, H. Kawamura, S. Miyakawa, P. Layrolle, N. Kanzaki, G. Treboux, K. Onuma, S. Tsutsumi, J. Biomed. Mater. Res. 60 (2002) 224.
[46] Y. Sogo, T. Sakurai, K. Onuma, A. Ito, J. Biomed. Mater. Res. 62 (2002) 457.
[47] H. Kawamura, A. Ito, T. Muramatsu, S. Miyakawa, N. Ochiai, T. Tateishi, J. Biomed. Mater. Res. 65A (2003) 468.
[48] M. Ikeuchi, A. Ito, Y. Dohi, H. Ohgushi, H. Shimaoka, K. Yonemasu, T. Tateishi, J. Biomed. Mater. Res. 67A (2003) 1115.
[49] Y. Sogo, A. Ito, M. Kamo, T. Sakurai, K. Onuma, N. Ichinose, M. Otsuka, R.Z. LeGeros, Mater. Sci. Eng., C 24 (2004) 709.
[50] M. Otsuka, Y. Ohshita, S. Marunaka, Y. Matsuda, A. Ito, N. Ichinose, K. Otsuka, W.I. Higuchi, J. Biomed. Mater. Res. 69A (2004) 552.
[51] A. Ito, M. Otsuka, H. Kawamura, M. Ikeuchi, H. Ohgushi, Y. Sogo, N. Ichinose, Curr. Appl. Phys. 5 (2005) 402.
[52] P. Layrolle, A. Ito, T. Tateishi, J. Am. Ceram. Soc. 81 (1998) 1421.
[53] L. Yubao, Z. Xingdong, K. de Groot, Biomaterials 18 (1997) 737.
[54] T. Ivanova, O.V.F. Kamenetskaya, A.B. Koltsov, V.L. Ugolkov, J. Solid State Chem. 160 (2001) 340.
[55] A.C. Tas, F. Korkusuz, M. Timucin, N. Akkas, J. Mater. Sci. Mater Med. 8 (1997) 91.
[56] I.R. Gibson, I. Rehman, S.M. Best, W. Bonfield, J. Mater. Sci. Mater. Med. 12 (2000) 799.
[57] B.S. Moonga, D.W. Dempster, J. Bone Miner. Res. 10 (1995) 453.
[58] S. Loher, W.J. Stark, M. Maciejewski, A. Baiker, S.E. Pratsinis, D. Reichardt, F. Maspero, F. Krumeich, D. Gunther, Chem. Mater. 17 (2005) 36.
[59] F. Miyaji, Y. Kono, Y. Suyama, Mater. Res. Bull. 40 (2005) 209.
[60] H. Storrie, S.I. Stupp, Biomaterials 26 (2005) 5492.
[61] X. Yin, L. Calderin, M.J. Stott, M. Sayer, Biomaterials 23 (2002) 4155.
[62] E. Chassot, H. Oudadesse, J. Irigaray, E. Curis, S. Benazeth, I. Nicolis, J. Appl. Phys. 90 (2001) 6440.